Large-Area Deployable Reflectarray Antenna for CubeSats

Manan Arya,* Jonathan Sauder,† Richard E. Hodges,‡
Jet Propulsion Laboratory, California Institute of Technology, 4800 Oak Grove Dr, Pasadena, CA 91109
and Sergio Pellegrino§
California Institute of Technology, 1200 East California Blvd, Pasadena, CA 91125

Herein is described a 1.5 m × 1.5 m reflectarray antenna designed to stow in a cylinder of 20 cm diameter and 9 cm height, and then be unfolded to provide an aperture suitable for radio frequency (RF) operations at X-band (8.4 GHz) and produce 39.6 dB of gain. The mass of the reflectarray, as measured for a full-scale prototype, is 1.75 kg. The reflectarray comprises a number of crossed-dipoles held 5 mm above a ground plane. The dipole layer and the ground plane are supported by thin planar composite facesheets; the separation between these facesheets is provided by thin composite collapsible 'S'-shaped-springs. The structure is divided into a number of quartz-epoxy composite strips arranged in concentric squares and connected to each other using slipping folds. The strips can be flattened, star-folded, and wrapped to package within the compact cylindrical volume. A full-scale prototype of this reflectarray was constructed and tested. Stowage in the design volume was successfully demonstrated, and all RF performance requirements were met, as shown by a pre-stowage RF test and a post-stowage RF test.

I. Introduction

There is great interest in designing large radio frequency (RF) apertures for small satellites such as CubeSats. Larger apertures will enhance the capabilities of small spacecraft by enabling higher data rate telecommunications and higher performance remote sensing instruments. Since the launch volume of CubeSats is limited, deployable apertures are used. Several deployable RF CubeSat apertures have been developed, to varying levels of technological maturity.[1–8] Key parameters of these developments are listed in Table 1; three of these aperture technologies are shown in Figure 1.

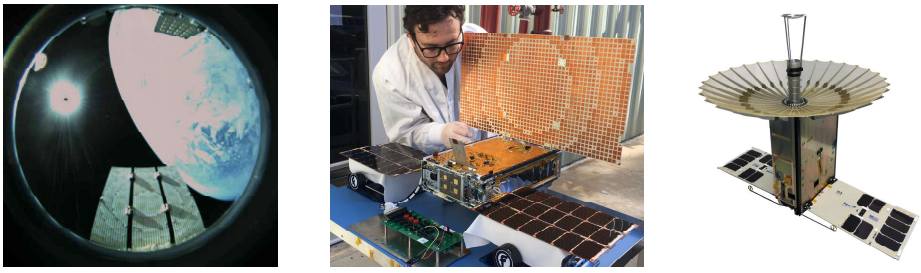

(a) (b) (c)

Figure 1: RF CubeSat apertures that have been successfully deployed in space. (a) ISARA (Integrated Solar Array and Reflectarray Antenna) experiment, (b) the MarCO (Mars Cube One) High-Gain Antenna (HGA), and (c) the RainCube KaPDA (Ka-band Parabolic Deployable Antenna) reflector.

*Technologist, Advanced Deployable Structures. AIAA Member. Manan.Arya@jpl.nasa.gov
†Technologist, Technology Infusion. AIAA Member. Jonathan.Sauder@jpl.nasa.gov
‡RF Microwave Engineer, Flight Communications Systems. Richard.E.Hodges@jpl.nasa.gov
§Joyce and Kent Kresa Professor of Aerospace and Civil Engineering, Graduate Aerospace Laboratories. AIAA Fellow. sergiop@caltech.edu

Two mechanical design architectures are dominant for deployable RF reflectors for small satellites: parabolic mesh antennas (e.g. KaPDA for RainCube,[2] KaTENna[7]), and planar reflectarrays (e.g. ISARA,[6] the MarCO High-Gain Antenna,[5] OMERA,[8] DaHGR[3]). A key example of a CubeSat RF aperture that is not a reflector is the S-band 1.24 m × 1.24 m patch array of antennas developed by Warren et al.[1]

	Aperture size	**Frequency**	**TRL**
ISARA	0.33 m × 0.27 m	26 GHz	9
MarCO HGA	0.60 m × 0.33 m	8.4 GHz	9
KaPDA	0.5 m diameter	36 GHz	9
DaHGR	0.6 m diameter	10 GHz	4-5
OMERA	1.05 m × 0.91 m	36 GHz	4-5
KaTENna	1 m diameter	36 GHz	4-5
Warren et al.	1.24 m × 1.24 m	3.6 GHz	4-5

Table 1: Key parameters of existing deployable RF apertures for CubeSats.

There is a need to develop larger apertures still, and this effort seeks to demonstrate the next generation of stowable planar reflectarray technology. The design proposed herein is capable of providing a 1.5 m × 1.5 m aperture that can be stowed in a cylindrical volume of 20 cm diameter and 9 cm height. As such, this reflectarray could be stowed in a 4U CubeSat volume. (A 'U' or a CubeSat unit refers to a cubical volume with 10 cm sides.) Note that additional volume will be required for the stowage of associated deployment hardware e.g. booms.

Figure 2 shows an overview of the Large-Area Deployable Reflectarray (LADeR) concept. The reflectarray, in gold, is supported by four deployable booms and connected to the CubeSat bus. A deployable RF feed is attached to the CubeSat bus, as well. This paper focuses exclusively on the design of the reflectarray subsystem; the supporting booms and the deployable feed may be adapted from existing designs (e.g. deployable TRAC booms[9] on NanoSail-D[10]). Also, this paper does not focus on the deployment of the reflectarray; previous efforts have demonstrated autonomous and controlled deployment of similar structures at relevant scales.[11]

The key developments described herein are of a novel RF design for a reflectarray, and a novel substrate that supports the reflectarray. The substrate is a collapsible structure that is lighter and more compactable than the solid substrates used for the MarCO HGA and ISARA, and also stiffer and capable of a higher degree of planarity than the creased polymer membrane substrates used by Warren et al. and DaHGR.

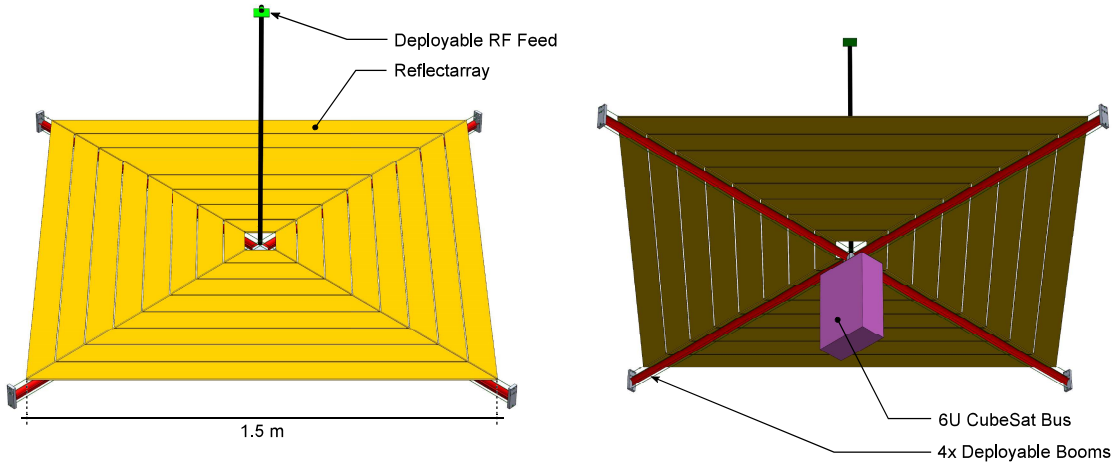

Figure 2: A conceptual illustration of LADeR deployed as part of an RF system from a 6U CubeSat.

This paper is arranged thus: Section II discusses the RF and structural design of the reflectarray antenna, and details the packaging concept for the antenna. Section III explains the fabrication process for a foldable, RF-capable prototype, and Section IV details the RF and packaging tests conducted on this prototype. Finally, Section V offers some conclusions.

II. Antenna Design

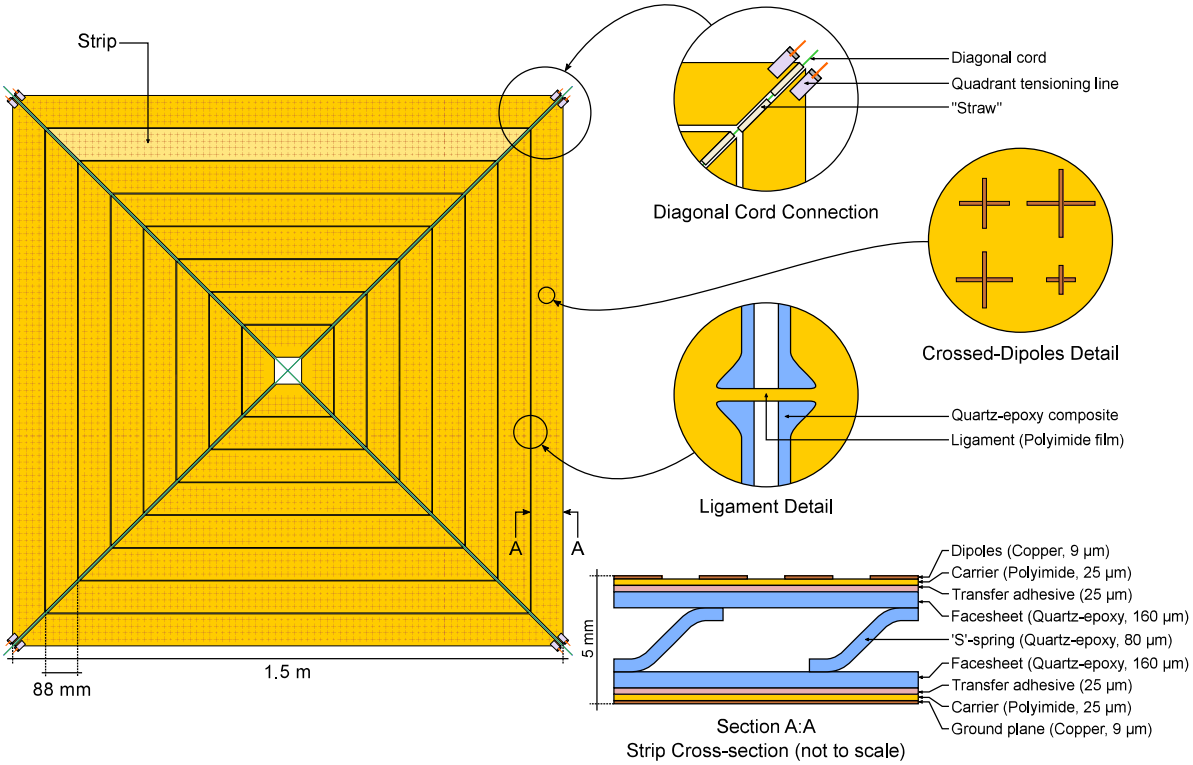

Figure 3: LADeR overview. A single strip is highlighted in the top quadrant for clarity.

II.A. RF Design

The reflectarray is comprised of 4340 cross-dipole elements spaced 22.5 mm apart in a rectangular lattice that forms a 1.5 m × 1.5 m reflector as illustrated in Figure 3. The reflector is illuminated by a feed placed at the focal point 1 m above the reflector surface along the central reflector axis, resulting in an F/D of 0.67. The dipoles lengths are adjusted in order to change the phase of the reflected signal, thereby collimating the energy that emanates from the feed. Packaging this concept to fit on a spacecraft as illustrated in Figure 2 requires a small feed and subreflector assembly mounted to a telescopic waveguide deployment mechanism. However, since the goal of this project was to demonstrate the deployable reflector technology, to save cost we instead used a small pyramidal horn with a 10 dB beamwidth of approximately 74°. The design of a combined feed and subreflector that provides similar illumination and has already been developed and proven for previous projects.[2]

The copper cross-dipole elements are photo etched on 25 µm-thick polyimide sheets bonded to an Astro-Quartz (AQ) facesheet, see Section A:A in Figure 3. These AQ sheets are supported above a copper ground plane using 'S'-springs. The details of this construction are described below in Section II.B. An important practical consideration in this design is that the fabrication process does not provide high-precision tolerances in several key dimensional parameters, and we do not have high accuracy knowledge of the material dielectric constants. To accommodate this, cross-dipole elements are placed 5 mm above the ground plane. Note that dielectrics in intimate contact with a cross-dipole element have a strong "loading" effect that will influence their resonant frequency, but this dielectric loading effect decays very rapidly as the dielectric sheets are moved away from the dipole. By supporting the dipoles on thin sheets, the dipoles are primarily influenced by the well-controlled properties of the polyimide layer, while other dielectrics have less impact. Also, the relatively large 5 mm dipole-to-ground plane separation was selected to provide a good range of achievable phase shifts while being relatively insensitive to dimensional tolerance. Consequently, this arrangement provides a robust, low-mass-density design that minimizes RF dielectric losses.

II.B. Structural Design

The reflectarray structure provides two planar parallel surfaces, separated by 5 mm, on which the antenna dipole layer and the ground plane reside. This separation is given by the basic structural unit of this reflectarray, which is a *strip*. As shown in Section A:A in Figure 3, a strip consists of two facesheets separated by a number of collapsible 'S'-shaped springs. Each facesheet is 160 µm thick, and is made of epoxy reinforced with woven quartz fabric. The 'S'-springs are 80 µm thick, and also made of the quartz-epoxy composite material. The antenna dipoles and ground plane, each of which consist of a layer of copper supported by a carrier layer of polyimide film, are adhered to the quartz-epoxy composite structure using transfer adhesive.

Because of its out-of-plane depth, a strip has substantial out-of-plane bending stiffness. This strip bending stiffness contributes to the stiffness of the overall array and is critical in maintaining the planarity of the reflectarray. Additionally, the cross-section of a strip allows it to be flattened elastically for packaging. An 'S'-spring consists of three flat sections connected by two transversely curved sections; the two transversely curved sections flex during flattening. The radius of curvature of the transversely curved sections is 5 mm, which ensures that the flattening strain on the 'S'-springs is less than 0.8 %, which is within the elastic regime of the strip material. (The flattening strain can be calculated as half the thickness of the 'S'-springs (80 µm) divided by the change in transverse radius (5 mm).)

The strip material, epoxy resin reinforced with woven quartz fibers, was chosen for its dielectric properties, its heritage in space reflector structures, its toughness, and its strength. Specifically, Patz PMT-F4 (a 120 °C-cure epoxy resin) and plain weave AstroQuartz II 525 were used. The fiber layups are as follows: two plies arranged in a [+45°/-45°] stack for the facesheets, and a single ply arranged in a [+45°] orientation for the 'S'-springs. (0° is defined as being along the length of the strip in this system.)

The antenna dipoles and the ground plane consist of a DuPont™Pyralux® material; this material comprises a layer of 25 µm-thick polyimide film clad with a layer of 9 µm-thick copper. The antenna dipoles were manufactured by a photolithography process, selectively chemically etching away the copper layer, leaving the desired arrangement of dipoles intact. The dipole layer and the ground plane were attached to the strip quartz-epoxy substrate using transfer adhesive, which was roughly 25 µm thick.

As shown in Figure 3, the strips are arranged in concentric squares. Two diagonal lines divide the array into four mechanically identical quadrants. In each quadrant, there are eight strips. Each strip is 88 mm in width; the length of the strip varies from 1.5 m at the outer edge of the array to 60 mm at the inner edge near the center. There are 2 mm gaps between the strips, which allow for a structural connection to exist between the strips. This specific arrangement of the strips is designed to allow for the stowing of the reflectarray, as further explained in Section II.C.

The structural architecture of this reflectarray is based on previous work.[11,12] The strips, each of which has non-negligible out-of-plane bending stiffness, are "hung" on two pretensioned cords that run along the diagonals of the reflectarray. These diagonal cords are pretensioned by deployable booms (see Figure 2); in the experiments described herein, the booms were substituted for a non-deployable cross of PVC tubing (see Figure 7). The structural connection between a strip and a diagonal cord consists of a "straw" of fabric tubing that is attached to the end of the strip; the tensioned diagonal cord passes through this "straw". In the prototype constructed for this effort, the diagonal cords were realized as braided Kevlar threads, tensioned by tightening a turnbuckle engaged in series with the cord.

In addition to the diagonal cords, the strips within a quadrant are also connected to each other through *slipping folds*. This type of fold allows for both rotation about and translation along the hinge axis. In this reflectarray, these slipping folds are realized as a number of *ligaments* between the strips (see Figure 3). To enable creaseless folding, the Pyralux material is mostly cut between the strips; the ligaments are lengths of uncut Pyralux. This allows for the relative folding and sliding of strips that is required for packaging, but maintains a degree of structural connectivity between the strips.

From a structural perspective, this reflectarray reacts in-plane loads through the in-plane tensile and compressive stiffness of the strips, and the pre-tension in the diagonal cords. Out-of-plane loads are reacted by the out-of-plane stiffness of the strips, and the pre-tension in the diagonal cords. Previous work[11,12] has established analytical and numerical models for predicting the stiffness of such structures. When deployed, the structure is sufficiently stiff to maintain its shape in 1g environment (positioned vertically, so gravity acts in the plane of the structure) without any gravity-offloading mechanisms.

The mass of the prototype reflectarray was measured to be 1.75 kg; this corresponds to an areal density of 779 $\mathrm{g\,m^{-2}}$. Table 2 lists the masses of the prototype components.

Component	Mass (g)	Source
Strip substrate	1171	Using measured strip linear density of $46.9\,\mathrm{g\,m^{-1}}$
Dipole layer	116	Using measured etched Pyralux areal density of $51.6\,\mathrm{g\,m^{-2}}$
Ground plane	261	Using measured unetched Pyralux areal density of $116.1\,\mathrm{g\,m^{-2}}$
Diagonal cords	5	Measured
Adhesive, tapes, etc.	197	Remainder of measured prototype mass
Total	1750	Measured prototype mass

Table 2: Mass breakdown of the prototype reflectarray.

II.C. Packaging Concept

The packaging concept is based on previous work on *slip-wrapping*.[11–13] The strips are connected by slipping hinges that allow the strips to rotate about and translate along the hinge axis. This allows the strips to be *star-folded*, and then wrapped into a compact form, as shown in Figure 4. Note that while Figure 4 shows a structure with 5 strips per quadrant, the current reflectarray design has 8 strips per quadrant; the general packaging concept, however, is unchanged: the strips are first flattened and folded into a star-like configuration with 4 arms, and the arms are then wrapped around each other. The folding of the strips is concurrent with the flattening of the strips. This flattening in crucial; without it, the strips would be unable to wrap tightly.

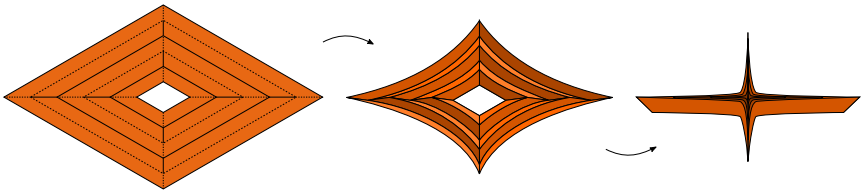

(a) Folding

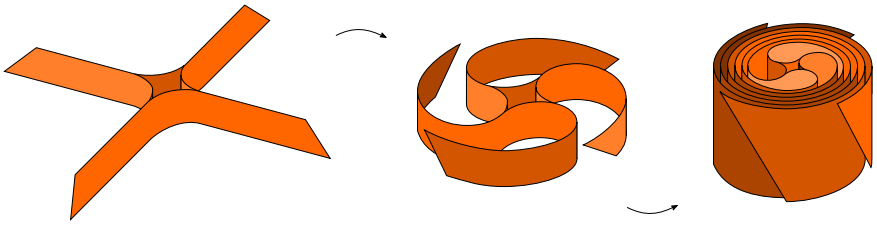

(b) Wrapping

Figure 4: Star folding and wrapping, illustrated for the case of 5 strips per quadrant. For clarity, only the outermost strips are shown in (b).

The slipping hinges allow the strips to slip with respect to each other during wrapping. This slip is required to accommodate the finite (non-zero) thickness of the flattened strip. By restricting the minimum radius R_{min} during wrapping (and thus the maximum curvature), the strains during wrapping can be restricted to be within the elastic range of the material. Thus the packaging can be an entirely elastic process, with no permanent damage or deformation of the strip structure. This allows the reflectarray to return to its original shape after deployment.

Figure 5 shows the predicted wrapped cross-section of this reflectarray for a minimum wrapping radius of 25.4 mm. Given the measured flattened strip thickness of 610 µm, the maximum strain in the wrapped strips can be estimated as the half the thickness divided by the radius, which is 1.2%. This is well below the compressive failure strain of the quartz-epoxy composite material of 1.9%.[14]

The predicted wrapped form of the reflectarray in Figure 5 was generated by a previously described algorithm[12] that models the wrapped strips as parallel spiral curves, separated from each other by distances to account for the non-zero material thickness.

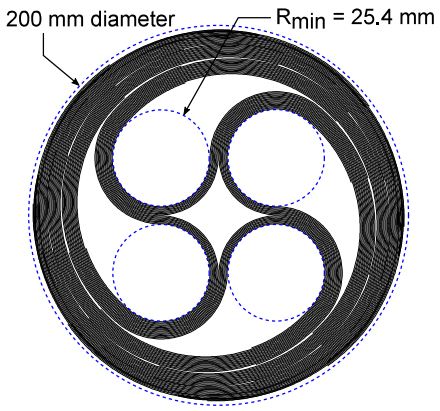

Figure 5: Predicted cross-section of the wrapped reflectarray.

III. Fabrication

The quartz-epoxy substrate of each strip was manufactured in 1.5 m lengths in a novel single-cure process in an oven.[15] Plain weave AstroQuartz (AQ) II 525 was impregnated with Patz PMT-F4 epoxy resin at roughly 40% resin content by Patz Materials & Technologies. The AQ prepreg was laid up in the desired configuration, with five custom-made silicone molds supporting the AQ prepreg, as shown in Figure 6. The silicone molds and the AQ were held in a five-piece aluminum encasement, held together with steel bolts. This encasement was necessary to constrain the high-coefficient-of-thermal-expansion (CTE) silicone molds during the 120 °C cure. Also because of this high CTE, the silicone expansion against the aluminum encasement provided sufficient pressure to cure the epoxy in the prepreg. As such, even though this process was conducted in an autoclave, the pressurization functionality of the autoclave was not required, and the autoclave functioned merely as an oven. Future fabrication activities could be carried out in long ovens, as opposed to autoclaves.

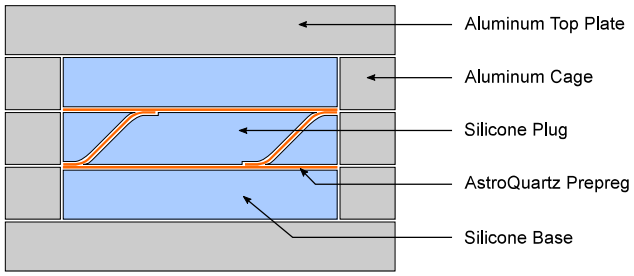

Figure 6: Cross-section of the molds used to fabricate a strip substrate.

20 lengths of strip substrate, each 1.5 m long, were manufactured. These lengths were then cut into the required shapes, forming the 32 strips of lengths ranging from 0.24 m to 1.50 m.

Once cut into the desired shapes, a layer of Pyralux was attached to the bottom facesheet of the strips using transfer adhesive. This formed the ground plane for each strip. Note that the ground plane is not continuous across all strips; separate trapezoids of Pyralux were attached to the bottom facesheet of each strip. Pyralux AC 092500EV was used for both the ground plane and the dipole layer.

To form the dipole layer, eight separate sheets (two sheets per reflectarray quadrant) of Pyralux were photolithographically etched by Pioneer Circuits. Pioneer Circuits also used a laser cutter to cut the sheets to size and to cut the ligaments into the material. For each quadrant, the two dipole layer sheets of etched and cut Pyralux were laid flat on a table, and the strip substrates were attached to the sheets using transfer adhesive.

The "straws" that connect the ends of the strips to the diagonal cords were 50 mm-long segments of flexible electrical-insulating sleeving made of woven fiberglass coated with acrylic plastic. These straws were about 3.3 mm in outer diameter, and flexible enough to fold and wrap with the strips. A straw was attached

to either end of a strip using fabric-reinforced adhesive tape. The diagonal cords, made of a braided Kevlar thread, were passed through these straws.

For the RF tests, the reflectarray was held in a deployed state using a cross made of 1-inch-diameter PVC tubing to simulate the four deployable booms shown in Figure 2. This cross was then mounted on a frame constructed from Bosch/Rexroth T-slot aluminum framing. Turnbuckles were used to tension the diagonal cords to an appropriate level, roughly 10 pounds of tension.

IV. Testing and Results

The prototype reflectarray was tested for RF performance and for packaging. The first RF test, RF Test 1, was performed before the prototype was packaged; this test was designed to evaluate the RF performance of a pristine (i.e. unfolded) reflectarray. Following RF Test 1, the reflectarray was stowed and deployed for Packaging Test 1. A second RF test, RF Test 2, was then performed to evaluate changes in RF performance due to the packaging process. Then, a final packaging test, Packaging Test 2, was performed.

IV.A. RF Tests

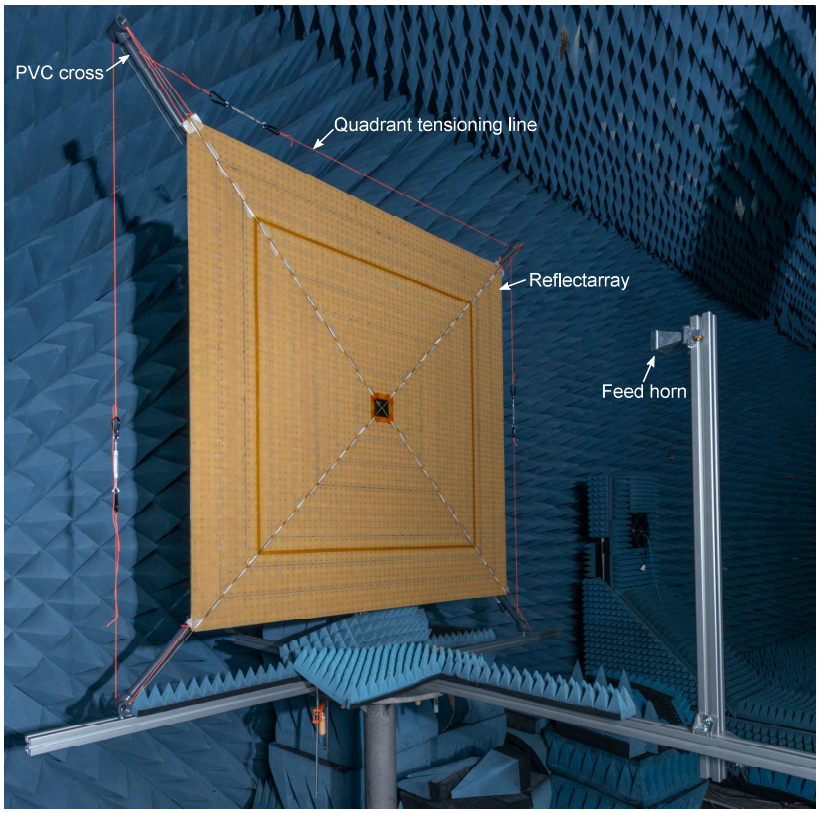

Figure 7: Configuration for the RF tests.

RF Test 1 was conducted at the JPL Mesa facility, using a planar near-field range. Figure 7 shows the prototype set up in a RF test chamber. The antenna prototype was held vertically, with gravity acting in the plane of the reflectarray. The PVC cross was clamped to a fixture in the range. An X-band horn, mounted at the focal point of reflectarray, 1 m ahead of the dipole layer, was used to illuminate the array for testing. The foldable prototype produced a peak of 39.6 dB of gain at 8.4 GHz.

RF Test 2 was conducted after a stow and deploy cycle to determine the effects of folding and unfolding on the RF performance. This test was conducted at NSI-MI Technologies, Inc. in Torrance, California, using a vertical planar near-field range. The test setup was comparable to the setup for RF Test 1. The planar ranges in both facilities use similar hardware, which is provided by NSI-MI Technologies.

Figure 8 shows the frequency-dependent measured gain of the reflectarray for both RF tests. As can

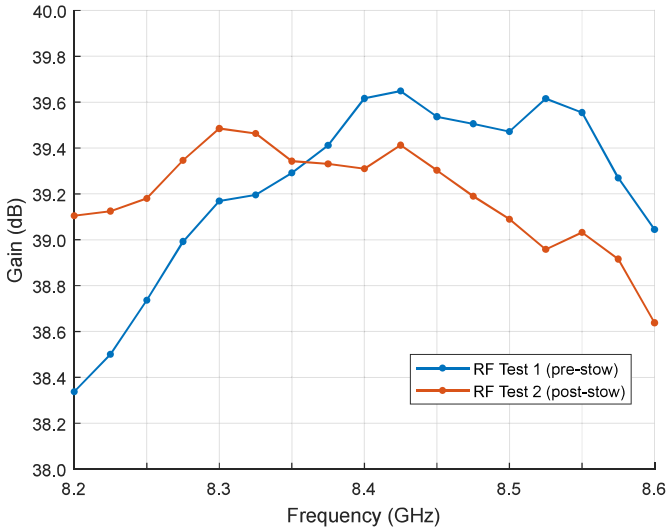

Figure 8: Measured RF gain.

be seen, stowing the reflectarray has very little effect on the gain produced by the antenna; the peak gain dropped by about 0.3 dB, and the peak frequency shifted by about 100 MHz. Figure 9 shows the measured beam patterns from RF Test 2. As can be seen, the reflectarray produced a well-focused beam in both azimuth and elevation, with low sidelobe levels.

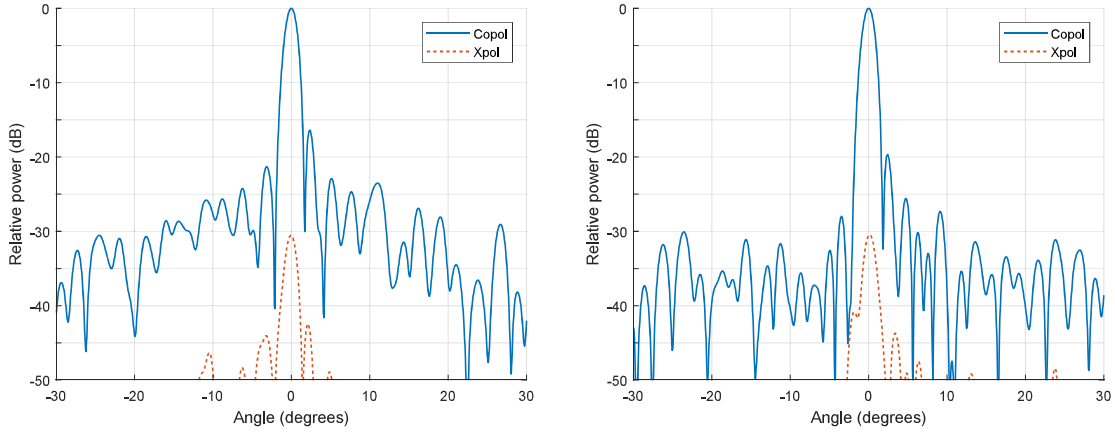

(a) Azimuth (b) Elevation

Figure 9: Measured antenna beam patterns from RF Test 2.

IV.B. Packaging Tests

The reflectarray was packaged manually. Figure 10 shows the packaging sequence. The deployed reflectarray was placed on a flat steel-top table 1.5 m in width. The strips were "star-folded" manually; the mountain folds were folded from the outside in. During this folding process, the strips were flattened. Bobby pins and large binder clips were used to hold the quadrants and the diagonals folded.

For the second step of wrapping, the star-folded reflectarray was placed in the middle of four aluminum tubes of known outer radius. The tubes limited the maximum curvature in the wrapped reflectarray. The outer radius of these tubes was 31.75 mm for the first packaging test, and 25.4 mm for the second. These four tubes were placed a known distance apart using shoulder bolts inserted in the steel-top table. The folded reflectarray was then manually wrapped around these four tubes. Once fully wrapped, the wrapped array

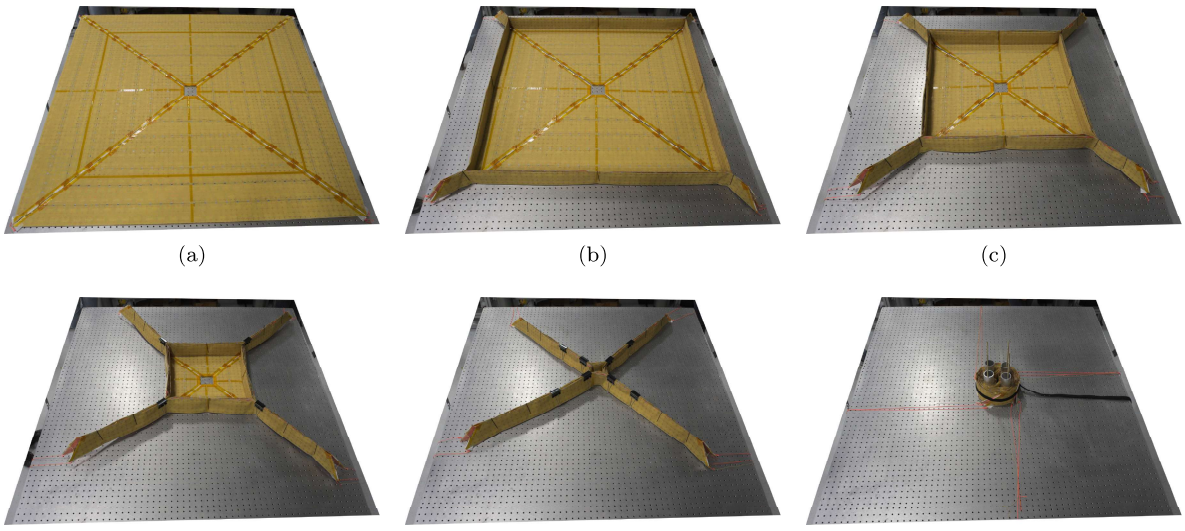

Figure 10: Packaging process. (a)-(e) shows the folding steps, and (f) shows the reflectarray fully wrapped. All images are shown at the same scale.

was held in place by a Velcro strap placed around the outer circumference of the wrapped structure. Figure 11 shows a plan view of the wrapped reflectarray after Packaging Test 2.

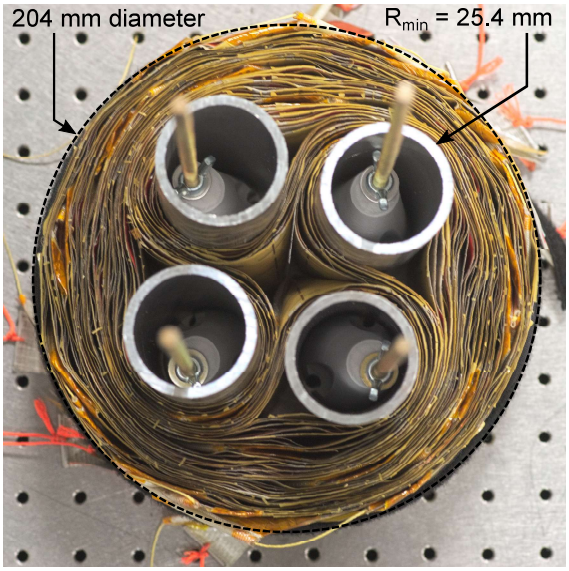

Figure 11: The fully packaged prototype at the end of the Packaging Test 2.

Once wrapped, the outer circumference of the reflectarray was measured using a flexible tape measure. From this, the packaged diameter was derived to be 241 mm for the first test, and 204 mm for the second test. The packaged height was around the strip width, about 88 mm. Table 3 shows the results of the two packaging tests, compared to predictions generated by a previously described algorithm.[12] Here, packaging efficiency η is the fraction of the cylindrical packaged volume occupied by the material of reflectarray. This cylindrical packaging volume $V_{packaged}$ was taken to have a height of the strip width 88 mm, and the radius as measured. The material volume $V_{material}$ was calculated as the area of the reflectarray A times the measured flattened strip thickness $h = 610\,\mu\text{m}$.

$$\eta = \frac{V_{material}}{V_{packaged}} = \frac{Ah}{\pi R_{packaged}^2 H_{packaged}} \tag{1}$$

	R_{min} (mm)	Packaged diameter (mm) Measured	Predicted	Packaging efficiency η Measured	Predicted
Packaging Test 1	31.75	241 ± 4	217	34.1%	42.1%
Packaging Test 2	25.40	204 ± 1	194	47.6%	52.7%

Table 3: Packaging test results.

It can be seen that the there is a close match between the predicted and measured packaged sizes, though the predicted diameters are consistently smaller than the measured, and the predicted packaging efficiencies are consistently larger than the measured values. It is expected that a more careful, less manual, and more predictable packaging method, either by using a jig or a mechanism to package the structure will yield packaged diameters and packaging efficiencies closer to the predicted values.

IV.C. Surface Flatness

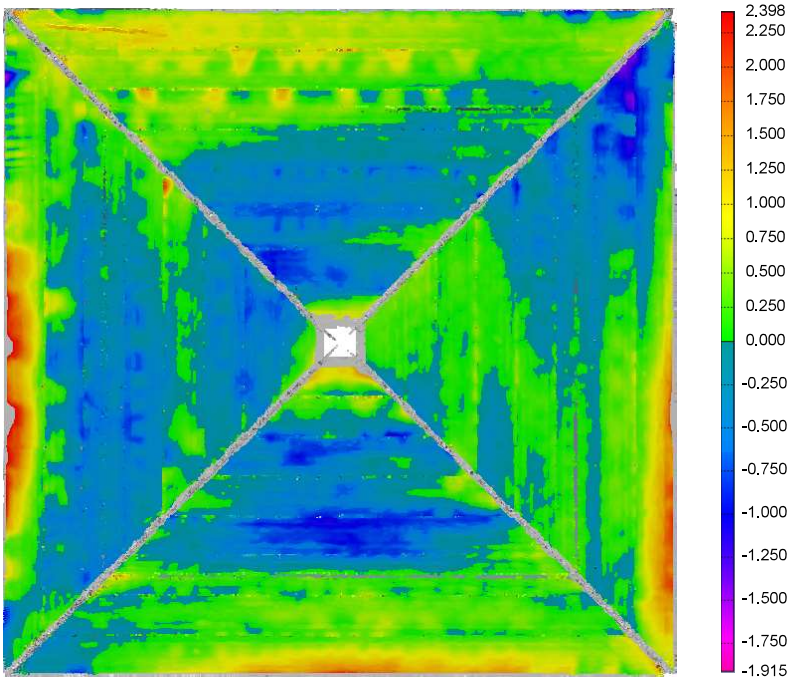

Figure 12: Surface flatness measurement before folding, after the RF test. The RMS is 0.5 mm. The colorbar units are millimeters.

The surface profile of the reflectarray was measured using a non-contact coordinate measuring machine (CMM). Specifically, a FARO arm with a laser-line scanner (which provides a measurement accuracy of roughly 50 µm) was used to scan the entire front surface of the deployed reflectarray. The results from this scan can be seen in Figure 12. This scan was performed after RF Test 1, and before Packaging Test 1. The measured surface RMS was 0.5 mm, much below the $\lambda/20 = 1.78$ mm surface RMS criterion generally applied to RF apertures. As can be seen, the bulk of the aplanarity of the array is concentrated on the outer edges.

V. Conclusions

We have developed a large-area deployable reflectarray antenna aperture capable of providing a 1.5 m × 1.5 m surface, but which can stow compactly in a 6U CubeSat. It consists of bending-stiff strips made of thin composite materials that can be flattened, folded, and wrapped. Since they are wrapped without permanent deformation, they can pop-up after deployment to provide separation between the reflectarray dipoles and the ground plane, and also provide increased bending-stiffness. The reflectarray itself consists of an array of crossed-dipoles.

This reflectarray antenna design promises apertures with much larger areas than existing state-of-the-art CubeSat deployable reflectors. It is also possible that this design can be scaled to larger sizes.

Acknowledgments

Arthur Schlothauer provided important input in the design of the manufacturing processes for the quartz-epoxy composite structures. Alexander Cheikh assisted with the fabrication of the strip substrates. Christopher Esquer-Rosas, Kenzo Neff, Serena Ferraro, Evan Hilgemann, Christine Gebara, Allison Ayad, Wiriya Poungparam, and Robert Salazar assisted with the assembly and the folding of the RF prototype. Juan Meija-Ariza assisted with the manufacturing of a non-deployable prototype. Jefferson Harrell conducted the pre-folding RF Test 1 at the JPL Mesa facility, and Stanley Fletcher conducted the post-folding RF Test 2 at NSI-MI Technologies in Torrance, California. The authors are grateful for funding for the post-fold RF test, which was secured by Timothy O'Donnell and James Zumberge. A part of this research was funded through the internal Research and Technology Development program at JPL. This research was carried out at the Jet Propulsion Laboratory, California Institute of Technology, under a contract with the National Aeronautics and Space Administration.

References

[1]Warren, P. A., Steinbeck, J. W., Minelli, R. J., and Mueller, C., "Large, Deployable S-Band Antenna for a 6U Cubesat," *29th Annual AIAA/USU Conference on Small Satellites*, 2015.

[2]Chahat, N. E., Hodges, R. E., Sauder, J., Thomson, M., Peral, E., and Rahmat-Samii, Y., "CubeSat Deployable Ka-Band Mesh Reflector Antenna Development for Earth Science Missions," *IEEE Transactions on Antennas and Propagation*, Vol. 64, No. 6, 2016, pp. 2083–2093.

[3]Kelly, P. K., "A Scalable Deployable High Gain Antenna - DaHGR," *AIAA/USU Conference on Small Satellites*, 2016.

[4]Hodges, R. E., Hoppe, D. J., Radway, M. J., and Chahat, N. E., "Novel Deployable Reflectarray Antennas for CubeSat Communications," *2015 IEEE MTT-S International Microwave Symposium, IMS 2015*, 2015.

[5]Hodges, R. E., Chahat, N. E., Hoppe, D. J., and Vacchione, J. D., "A Deployable High-Gain Antenna Bound for Mars: Developing a new folded-panel reflectarray for the first CubeSat mission to Mars," *IEEE Antennas and Propagation Magazine*, Vol. 59, No. 2, 2017, pp. 39–49.

[6]Hodges, R. E., Lewis, D. K., Radway, M. J., Toorian, A. S., Aguirre, F. H., Hoppe, D. J., Shah, B. N., Gray, A. A., Rowen, D. W., Welle, R. P., Kalman, A. E., Reif, A. W., and Martin, J. M., "The ISARA Mission - Flight Demonstration of a High Gain Ka-Band Antenna for 100Mbps Telecom," *AIAA/USU Conference on Small Satellites*, 2018.

[7]Gao, S., Rahmat-Samii, Y., Hodges, R. E., and Yang, X.-X., "Advanced Antennas for Small Satellites," *Proceedings of the IEEE*, Vol. 106, No. 3, 2018, pp. 391–403.

[8]Chahat, N. E., Agnes, G., Sauder, J. F., and Cwik, T., "One Meter Deployable Reflectarray Antenna for Earth Science Radars," *2017 IEEE Antennas and Propagation Society International Symposium Proceedings*, 2017.

[9]Banik, J. A. and Murphey, T. W., "Performance Validation of the Triangular Rollable and Collapsible Mast," *24th Annual AIAA/USU Conference on Small Satellites*, 2010.

[10]Johnson, L., Whorton, M. S., Heaton, A., Pinson, R., Laue, G. P., and Adams, C. L., "NanoSail-D: A solar sail demonstration mission," *Sixth IAA Symposium on Realistic Near-Term Advanced Scientific Space Missions*, 2009.

[11]Arya, M., Lee, N., and Pellegrino, S., "Ultralight structures for space solar power satellites," *3rd AIAA Spacecraft Structures Conference*, 2016.

[12]Arya, M., *Packaging and Deployment of Large Planar Spacecraft Structures*, Ph.D. thesis, California Institute of Technology, 2016.

[13]Arya, M., Lee, N., and Pellegrino, S., "Crease-free biaxial packaging of thick membranes with slipping folds," *International Journal of Solids and Structures*, Vol. 108, 2017, pp. 24–39.

[14]Murphey, T. W., Francis, W. H., Davis, B. L., Meija-Ariza, J., Santer, M. J., Footdale, J. N., Schmid, K., Soykasap, O., Guidanean, K., and Warren, P. A., "High Strain Composites," *2nd AIAA Spacecraft Structures Conference*, 2015.

[15]Schlothauer, A., Royer, F., Pellegrino, S., and Ermanni, P., "Flexible Silicone Molds for the Rapid Manufacturing of ultra-thin Fiber Reinforced Structures," *Society for the Advancement of Material and Process Engineering (SAMPE 2018)*, 2018.